PERGAMON

Nonlinear Analysis 47 (2001) 5309–5324

Nonlinear Analysis

www.elsevier.nl/locate/na

On a Rent-Seeking Game described by a Non-Invertible Iterated Map with Denominator ⋆

Gian-Italo Bischi[a], Michael Kopel[b], Ahmad Naimzada[c]

[a] *Istituto di Scienze Economiche, University of Urbino, Italy.*
[b] *Department of Managerial Economics and Industrial Organization, University of Technology, Theresianumgasse 27, 1040 Vienna, Austria*
[c] *University "Bocconi", via Sarfatti, 20132 Milano, Italy.*

Abstract

A dynamic rent seeking game with two boundedly rational players is analyzed. The game is modeled as a discrete dynamical system of the plane, represented by the iteration of a noninvertible map with a denominator which vanishes in a one-dimensional subset of the plane and this gives rise to basins of attraction with particular structures, called *lobes* and *crescents* in [1]. These structures are related to the presence of a *focal point*, i.e. a point where the map assumes the form 0/0. We show that the focal point of this map has some peculiar properties which lead to situations not included in the cases described in [1].

Key words: Discrete dynamical systems, games, stability, noninvertible maps, basins of attraction

1 Introduction

Many interesting economic situations can be considered as rent-seeking contests, in which the contestants expend effort to win a prize. For example, firms compete to obtain a procurement contract from the government or by spending R&D expenditures to win a patent. See [2] for a survey of various applications. The basic rent-seeking contest considers N agents which are confronted with the opportunity to win a fixed prize R. If we let x_i denote the expenditure of

⋆ This work has been performed under the auspices of CNR, Italy, and under the National Research Project "Nonlinear Dynamics and Stochastic Models in Economics and Finance", financed by MURST, Italy.

0362-546X/01/$ - see front matter
PII: S0362-546X(01)00637-X

agent i (in units commensurate with the rent), then the probability that agent i wins the rent is $p_i(x_1, ..., x_N)$, where $\sum_{i=1}^{N} p_i = 1$ and p_i is nondecreasing in x_i and nonincreasing in $x_j, j \neq i$. A commonly used form of the probability functions in rent-seeking games is the logit type (see e.g. [3]), which specifies that agent i's probability for winning the rent is

$$p_i = \frac{f_i(x_i)}{\sum f_j(x_j)},$$

where $f_i(x_i), i = 1, ...N$ may be interpreted as the likelihood that agent i wins the contest when he expends effort x_i. It is usually assumed that $f_i(x_i)$ is twice differentiable, increasing and concave with $f_i(0) = 0$. If all the contestants do not expend any effort, we just simply define $p_i = 1/N \ \forall i$. The agents try to choose their efforts x_i to maximize their expected utility V_i. If we assume that the rent R is normalized to 1 and that all rent-seekers are risk-neutral, then

$$V_i = p_i(1 - x_i) + (1 - p_i)(-x_i) = p_i - x_i = \frac{f_i(x_i)}{\sum f_j(x_j)} - x_i.$$

Using the simple transformation $q_i = f(x_i)$, we can write the net rent of agent i as $\pi_i = \frac{q_i}{\sum q_j} - C_i(q_i)$,where C_i is the inverse of f_i. Note that both model formulations lead to identical analytical and qualitative results.

The literature on rent-seeking games has been primarily concerned with the existence and characterization of Nash equilibria – a situation, where no player can improve his/her expected profit by unilateral deviation from his/her equilibrium strategy – the effect of asymmetry in rent-seeker's characteristics and the relationship between total rent-seeking outlays in equilibrium and the value of the contested rent. See e.g. [3–6]. Less attention has been paid to dynamic issues which arise when the contestants are assumed to be only boundedly rational (for the notion of bounded rationality, see e.g. [7–9]). In fact, only recently issues like learning or adaptive behavior of the rent-seekers have been considered, where the focus has been on the issue of local stability. See [10–13]. However, no results concerning global stability or the delimitation of the basins of attractions of the stable Nash equilibria are given.

In this paper we try to move a step towards filling this gap. We consider a discrete time dynamic rent-seeking game where the agents compete repeatedly for the same prize each period. We assume that rent-seekers behave boundedly rational and adjust their efforts over time proportionally to their marginal profits, i.e.

$$q_i' = q_i + \alpha_i(q_i)\left[\frac{\partial \pi_i(q_1, q_2, ..., q_N)}{\partial q_i}\right], \quad i = 1, ..., N \tag{1}$$

where $\alpha_i(q_i)$ are positive functions. The unit-time advancement operator is denoted by $'$, i.e. if the right hand side includes variables at period t, then the left hand side represents the state variables at period $(t+1)$. An adjustment mechanism similar to (1) has been recently proposed by some authors (mainly in continuous-time formulations; see [13,11]).

A primary question in the literature on dynamic games is if the repeated interaction between the players will eventually lead to a Nash equilibrium in the long run despite the fact that these players act (only) boundedly rational in the short run. Traditionally, answers to this question have been given in terms of the local stability of Nash Equilibria. However, in the presence of other attracting sets (at finite or infinite distance), local stability is not enough. In a nonlinear model the basin of attraction of a locally stable equilibrium may be so small that any practical meaning of stability is lost. Consequently, only a study of the extension of the basin of a stable equilibrium can give information about its robustness with respect to exogenous perturbations. This requires a global analysis of the dynamical system (1), i.e. a study not based on linear approximations. Since for general higher-dimensional systems such results are hard to come by, we will limit ourselves to the case of two contestants. Hence, in what follows we will focus on a discrete dynamical system of the plane, represented by the iteration of a noninvertible map with denominator. This will give us the opportunity to apply some of the methods recently introduced in [1]. There the concepts of *focal points* and *prefocal curves* have been introduced to explain the creation of particular structures of the basins called *lobes* and *crescents*. As we will demonstrate, in our dynamic game such structures determine the qualitative properties of the basins. The focal point which is responsible for their appearance has some peculiar properties which lead to situations not included in the cases described in [1].

The paper is organized as follows. In Section 2 we give a brief summary of the local stability analysis. We turn to the global analysis of the dynamical system in section 3. We introduce the concept of critical curves (section 3.1) and focal points and prefocal sets (section 3.2). Finally, we apply these concepts to explain the structure of the basin of attraction in section 3.3.

2 Local stability analysis for a game with two players

We consider a model (1) with two players, where we assume linear costs, i.e. $C_i(q_i) = c_i q_i$, and linear functions $\alpha_i(q_i) = v_i q_i$, $i = 1, 2$. The latter assumption captures the fact that *relative effort variations* are proportional to marginal net rents, i.e.

$$\frac{q_i' - q_i}{q_i} = v_i \left(\frac{\partial \pi_i}{\partial q_i}\right)$$

where v_i is a positive constant which will be called *speed of adjustment.* With these assumptions (1) assumes the form $\left(q_1', q_2'\right) = T\left(q_1, q_2\right)$, where the map T is given by

$$T : \begin{cases} q_1' = q_1 \left(1 - c_1 v_1 + v_1 \frac{q_2}{(q_1+q_2)^2}\right) \\ \\ q_2' = q_2 \left(1 - c_2 v_2 + v_2 \frac{q_1}{(q_1+q_2)^2}\right) \end{cases} \tag{2}$$

Map T is not defined along the line $q_1+q_2 = 0$ (*line of non-definition* δ_s). Since the state variables q_1, q_2 represent the agents' efforts, we are only interested in the dynamics of (2) in the region $\mathbb{R}^2_+ = \{q_1, q_2 \,|\, q_1 \geq 0,\ q_2 \geq 0\}$. The only point of $\mathbb{R}^2_+$ belonging to the line δ_s is $(0,0)$. However, as we shall see in the next section, the presence of this point may have a crucial influence on the structure of the basins in $\mathbb{R}^2_+$.

A Nash equilibrium, if it exists, is also a stationary point of the dynamical system (1), located at the intersection of the reaction curves defined by $\partial\pi_i/\partial q_i = 0$, $i = 1, 2$. The steady states of the game are the non-negative fixed points of the map (2). It is immediate to see that a unique fixed point $E^* \notin \delta_s$ exists,

$$E^* = (q_1^*, q_2^*) = \left(\frac{c_2}{(c_1+c_2)^2}, \frac{c_1}{(c_1+c_2)^2}\right),$$

which is also the unique Nash equilibrium of the game. Following a standard stability analysis, a sufficient condition for the stability of E^* is that the eigenvalues of the Jacobian matrix $DT(q_1, q_2)$ of (2), computed at E^* are inside the unit circle of the complex plane. This is true if and only if the following conditions hold (see e.g. [14], p.159).

$$\begin{cases} 1 - Tr^* + Det^* = v_1 v_2 c_1 c_2 > 0 \\ \\ 1 + Tr^* + Det^* = c_1 c_2 v_1 v_2 - 4\frac{c_1 c_2}{c_1+c_2}(v_1 + v_2) + 4 > 0 \\ \\ Det^* - 1 \quad = \quad c_1 c_2 v_1 v_2 - 2\frac{c_1 c_2}{c_1+c_2}(v_1 + v_2) < 0 \end{cases} \tag{3}$$

where Tr^* and Det^* represent the trace and the determinant of $DT(E^*)$ respectively. The first condition is always satisfied, whereas the other two define a bounded region of stability in the parameter space. Given the unitary costs c_1 and c_2, the stability region can be represented in the plane $\mathcal{V} = \{v_1, v_2 \,|\, v_1 \geq 0, v_2 \geq 0\}$, as shown in fig. 1. This region is symmetric with respect to the diagonal $v_1 = v_2$ and bounded by the positive branches of two equilateral hyperbolae whose equations are obtained from the second and the third condition of (3). The coordinates of the vertices of this region are

$$A_1 = \left(\frac{2}{c_1}, \frac{2}{c_2}\right) \quad A_2 = \left(\frac{2}{c_2}, \frac{2}{c_1}\right) \quad B_1 = \left(\frac{c_1 + c_2}{c_1 c_2}, 0\right) \quad B_2 = \left(0, \frac{c_1 + c_2}{c_1 c_2}\right).$$

The rectangle $[0, 2/c_1] \times [0, 2/c_2]$ represents the region where only bounded trajectories can be obtained,i.e. no attractors at infinite distance exist (see the Appendix).

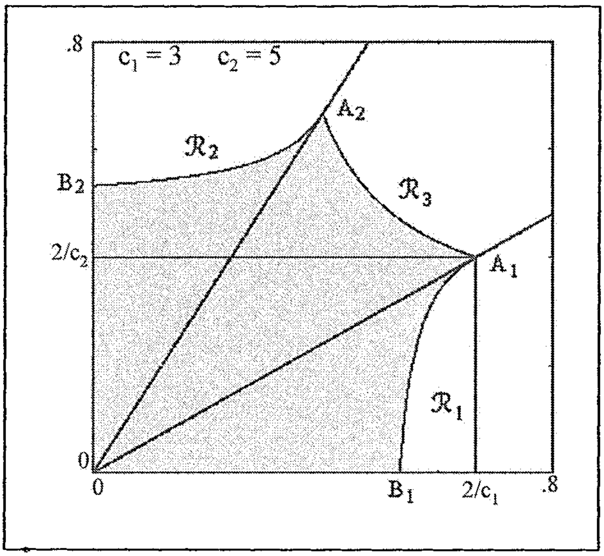

Figure 1.

The eigenvalues are complex conjugate if $(c_2 v_2 - c_1 v_1)(c_1 v_2 - c_2 v_1) < 0$, a condition which can be visualized in $\mathcal{V}$ as the region between the two lines $v_2 = \frac{c_1}{c_2} v_1$ *and* $v_2 = \frac{c_2}{c_1} v_1$. If $P = (v_1, v_2)$ crosses the boundary of the stability region along the arc $A_1 A_2$ (belonging to the hyperbola of equation $Det^* = 1$) then the fixed point E^* changes from a stable focus to an unstable focus via a Neimark-Hopf bifurcation, whereas if P exits the stability region by crossing one of the arcs $B_1 A_1$ or $B_2 A_2$ (both belonging to the other hyperbola given by equation $1 + Tr^* + Det^* = 0$) then the fixed point E^* changes from an attracting node to a saddle point through a period doubling (or flip) bifurcation.

We observe that if $c_1 = c_2$ then $A_1 \equiv A_2$, i.e. the region of stability in the space $\mathcal{V}$ becomes a square bounded by the branches of a degenerate hyperbola, and no Hopf bifurcations can occur. On the other hand, if the difference between the marginal costs of the two firms is increased, then the arc A_1A_2, representing the curve where Hopf bifurcations occur, becomes larger. This confirms an observation made in [13] (for dynamic rent-seeking games in continuous time) that only in the presence of a dominant agent the creation of limit cycles via Hopf bifurcation can occur. We finally remark that an increase of the speeds of adjustment has, in general, a destabilizing role. This property of adaptive adjustment processes has been observed before; see e.g. [15–17]). However, in our model with $c_1 \neq c_2$, the stability analysis reveals that, given E^* is unstable, stability of E^* can be obtained by increasing one (or both) parameters v_i. This happens when the point $P = (v_1, v_2)$ belongs to one of the regions denoted by $\mathcal{R}_1$ or $\mathcal{R}_2$ in fig. 1. Furthermore, if the point P moves from region $\mathcal{R}_1$ (or $\mathcal{R}_2$) to the region $\mathcal{R}_3$ due to a change in v_1 (or v_2), we obtain two bifurcations, which cause a transition from instability to instability separated by a "window" of stability.

3 Global study of the basins

The arguments given so far are based on local stability results. However, such insights may lead to misleading conclusions if they are not supported by an analysis of the basins of attraction. To illustrate, we present a situation where the Nash Equilibrium is locally stable, but the corresponding basin of attraction is quite small, as shown in fig. 2, where the white region represents the (numerically computed) basin of E^* and the grey region represents the basin of infinity[1]. The global dynamic properties of (2) and, in particular, the structure of the basins are strongly influenced by the following two features:

i) the map T is a *noninvertible map* of the plane, so its global geometric properties can be characterized by the method of *critical curves* (see [14,18])
ii) the map T has denominators which vanish along a one-dimensional subset of the plane, on which a *focal point* exists (see [1]).

[1] From an economic point of view, diverging trajectories do not represent interesting evolutions. As they can be interpreted as an irreversible departure from optimality, they might be excluded from the analysis of the economic model.

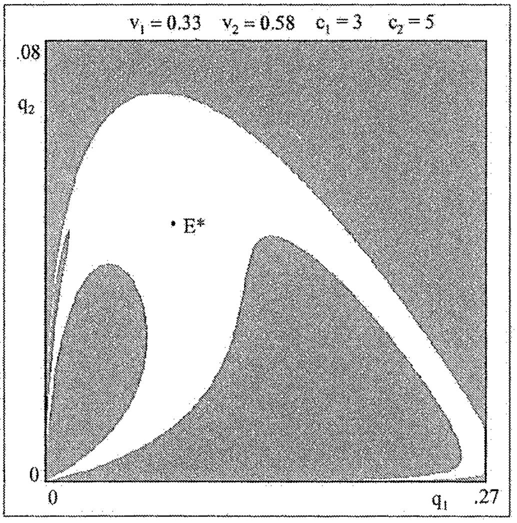

Figure 2.

3.1 *Critical curves*

A map T is noninvertible if distinct points exist which have the same image. The geometric action of a noninvertible map can be expressed by saying that it folds and pleats the phase space. Equivalently, we can say that a point may have several rank-1 preimages. The inverse relation T^{-1} may be multi-valued, given by the union of several inverse maps which "unfold" the phase space. The map T defined in (2) is noninvertible: calculating (q_1, q_2) in terms of a given (q_1', q_2') leads to a third degree algebraic system. So, as the point (q_1', q_2') varies in $\mathbb{R}^2$, the number of its rank-one preimages can be one or three. Accordingly, the plane can be subdivided into two regions, denoted by Z_1 and Z_3 (we follow the notations introduced in [18] and [19]) where one or three distinct inverses are defined respectively. Generally, pairs of real preimages appear or disappear as the point (q_1', q_2') crosses the boundary separating the regions Z_i. Such boundaries are characterized by the presence of two coincident preimages. This leads to the definition of the critical curves. The critical curve of rank-1, denoted by LC, is defined as the locus of points having two (or more) coincident rank-1 preimages, which are located on a set called LC_{-1}. LC is the two-dimensional generalization of the notion of critical value (local minimum or maximum value) of a one-dimensional map, LC_{-1} is the generalization of the notion of critical point (local extremum point). Arcs of LC separate the regions of the plane characterized by a different number of real preimages. When the map T is continuously differentiable, LC_{-1} is included in the set of points where the determinant of the Jacobian of T vanishes (i.e. in the set of points where T is not locally invertible):

$$LC_{-1} \subseteq \left\{ \mathbf{x} \in \mathbb{R}^2 |\ \det DT = 0 \right\}.$$

For (2) the points at which the determinant of the Jacobian vanishes can be easily computed, and $LC = T(LC_{-1})$ separates the region Z_3, where three distinct inverses, say T_1^{-1}, T_2^{-1} and T_3^{-1}, exist, from Z_1, where only T_3^{-1} is defined.

3.2 Focal point and prefocal set

Our dynamical system which is obtained by the iteration of T is defined on the plane deprived of the line of non-definition δ_s, as well as all their preimages of any rank, i.e. on the set

$$A = \mathbb{R}^2 \setminus \bigcup_{n=0}^{\infty} T^{-n} \left(\delta_s \right)$$

In fact, only points belonging to the set A generate feasible trajectories by the iteration of the map $T : A \to A$. Notice that, being δ_s a curve of $\mathbb{R}^2$, the set $\bigcup_{n \geq 0} T^{-n} \left(\delta_s \right)$ has zero Lebesgue measure in $\mathbb{R}^2$. The structure of the basins of (2) is strongly influenced by the presence of a so-called *focal point* Q, where the map assumes the form $0/0$ (for our game, $Q = (0, 0)$).

Definition (see [1]). *A point Q=(x_0,y_0) is a focal point if at least one component of the map T takes the form 0/0 in Q and there exist smooth simple arcs $\gamma(t)$, with $\gamma(0)$=Q, such that $\lim_{\tau \to 0} T(\gamma(\tau))$ is finite. The set of these finite values, obtained with different arcs $\gamma(t)$ through Q, is the prefocal set δ_Q.*

In [1] a map in the form $(x', y') = (F(x, y), N(x, y)/D(x, y))$ is considered. It is shown that if a focal point Q is simple, i.e. $\overline{N}_x \overline{D}_y - \overline{N}_y \overline{D}_x \neq 0$, where the terms with subscripts denote partial derivatives evaluated in (x_0, y_0), then the whole line $x = F(Q)$ is the corresponding prefocal curve δ_Q. Furthermore, it is proven that a one-to-one correspondence exists between the slope m of an arc γ through Q and the point $(F(Q), y)$ in which its image crosses δ_Q. This correspondence is given by

$$m \to (F(Q), y(m)), \qquad \text{with} \qquad y(m) = \frac{\overline{N_x} + m\overline{N_y}}{\overline{D_x} + m\overline{D_y}} \tag{4}$$

or, equivalently

$$(F(Q), y) \to m(y) \quad \text{with} \qquad m(y) = \frac{\overline{D_x}y - \overline{N_x}}{\overline{N_y} - \overline{D_y}y}. \tag{5}$$

The proof is based on considering a smooth simple arc γ transverse to δ_s, represented by

$$\gamma(\tau) : \begin{cases} x(\tau) = x_0 + \xi_1\tau + \xi_2\tau^2 + \dots \\ y(\tau) = y_0 + \eta_1\tau + \eta_2\tau^2 + \dots \end{cases} \qquad \tau \neq 0$$

crossing through Q, and assuming that $N(x,y)$ and $D(x,y)$ are smooth functions, so that

$$N(x,y) = \overline{N_x}(x - x_0) + \overline{N_y}(y - y_0) + O_2$$
$$D(x,y) = \overline{D_x}(x - x_0) + \overline{D_y}(y - y_0) + O_2'$$

where O_2 , O_2' represent terms of higher order. If Q is a simple focal point then

$$\lim_{\tau \to 0} \frac{N(\gamma(\tau))}{D(\gamma(\tau))} = \frac{\overline{N_x}\xi_1 + \overline{N_y}\eta_1}{\overline{D_x}\xi_1 + \overline{D_y}\eta_1}.$$

from which (4) and (5) follow, where $m = \eta_1/\xi_1$ is the slope of γ in Q.

This can also be stated by saying that at least one inverse of the map exists which maps any arc crossing δ_Q in y into an arc crossing through Q with slope $m(y)$. So, roughly speaking, a *prefocal curve* is a set of points for which one inverse exists which maps (or "focalizes") the whole set into the corresponding *focal point.* One conclusion here is of particular interest: if we consider the rank-1 preimage of an arc crossing δ_Q in *two* points $(F(Q), y_1)$ and $(F(Q), y_2)$, then at least one rank-1 preimage forms a *loop* with a knot in Q, with the two branches issuing from Q having slopes $m(y_1)$ and $m(y_2)$.

These properties are crucial for the global dynamical properties of a map T of the plane for the following reason. The boundary $\mathcal{F}$ of a basin is backward invariant, i.e. $T^{-1}(\mathcal{F}) = \mathcal{F}$, where here T^{-1} represents the set of all the inverses of T. Hence, if ω is a portion of $\mathcal{F}$, then all its preimages of any rank must belong to $\mathcal{F}$. This implies that if a portion ω of $\mathcal{F}$ has a tangential contact with a prefocal curve δ_Q and then it crosses δ_Q as some parameter is varied, the boundary $\mathcal{F}$ must contain a loop issuing from Q as well as loops issuing from the preimages of Q of any rank. The portions of the basins inside these loops have been called lobes in [1].

This mechanism which we described verbally causes the creation of the "finger-shaped" structure of the basin shown in fig. 2. Observe the lobes issuing from the focal point $Q = (0,0)$. However, in our case the situation is a bit more intricate than the one analyzed in [1]. In particular, the correspondence between slopes of arcs through Q and points of δ_Q is two-to-one. This is due to the fact that both components of the map (2) become 0/0 in Q, and Q is not simple. In fact, all the first partial derivatives of $N(q_1, q_2) = q_1 q_2$ and $D(q_1, q_2) = (q_1 + q_2)^2$ vanish in Q. Hence, the correspondence is obtained by considering second order terms in the expansions of N and D. This leads to

$$\lim_{\tau \to 0} T(\gamma(\tau)) = (v_1 u(m), v_2 u(m))$$
$$\text{with } u(m) = \frac{\overline{N}_{q_1q_1} + 2\overline{N}_{q_1q_2}m + \overline{N}_{q_2q_2}m^2}{\overline{D}_{q_1q_1} + 2\overline{D}_{q_1q_2}m + \overline{D}_{q_2q_2}m^2} = \frac{m}{(1+m)^2}$$

where $(-\infty, 1/4]$ is the range of the function $u(m)$. This expression defines a two-to-one correspondence between a point $\left(u, \frac{v_2}{v_1}u\right)$ along the line $q_2 = \frac{v_2}{v_1}q_1$ and the slopes of arcs through Q,

$$m_{\pm}(u) = \frac{(v_1 - 2u) \pm \sqrt{v_1^2 - 4v_1 u}}{2u}, \tag{6}$$

provided that $u < \frac{v_1}{4}$. Thus, the point Q is a focal point with prefocal set δ_Q given by the half-line $q_2 = \frac{v_2}{v_1}q_1$, where $q_1 \leq \frac{v_1}{4}$ with endpoint in $C = \left(\frac{v_1}{4}, \frac{v_2}{4}\right)$. Really, δ_Q may be considered as a line "folded into itself" in the point C as it appears from the analysis of the critical curves of (2). In fact, the points of the line $q_2 = \frac{v_2}{v_1}q_1$ above C belong to Z_1, so that they have only one rank-one preimage by T_3^{-1}, whereas the points of that line located below C belong to Z_3, so they have three rank-one preimages, two of which are "focalized" in the focal point Q, namely those obtained by T_1^{-1} and T_2^{-1}, whereas the third one, given by T_3^{-1}, belongs to the line $q_2 = \frac{(1-c_1v_1)v_2}{(1-c_2v_2)v_1}q_1$. The properties of the focal point Q and the set of focal values δ_Q are summarized by the following proposition:

Proposition. *Any arc η "crossing" δ_Q in a point $\left(u, \frac{v_2}{v_1}u\right)$, $u < \frac{v_1}{4}$, $u \neq 0$, has two distinct rank-one preimages "crossing" the focal point Q with slopes $m_{\pm}(u)$ given in 6). In particular, any arc η crossing δ_Q in the focal point Q has two distinct rank-one preimages which are tangent to the coordinate axes in Q (i.e. with slopes $m = 0$ and $m = \infty$).*

It is plain that if we consider an arc η crossing δ_Q in two points, then its rank-one preimages include two loops issuing from Q. The second part of the proposition strèsses another peculiarity of the map (2): the fact that $Q \in \delta_Q$. This gives rise to the following

Corollary. *Any arc transverse to δ_Q has infinitely many preimages which are arcs through Q with slopes* 0 and ∞ *in Q.*

Proof. Two preimages of an arc which crosses δ_Q are arcs through Q. But since $Q \in \delta_Q$, any arc through Q and transverse to δ_Q can be considered as a generic arc crossing δ_Q, and thus it has two rank-1 preimages again across δ_Q in Q. According to the relation (6) any arc through Q has two preimages through Q again, with slopes 0 and ∞ respectively, and so on, iteratively. □

This has important consequences on the structure of the basins of the dynamical system (2), as we shall see in the next section through some numerical explorations.

3.3 Lobes and crescents of $B(\infty)$.

We now study one particular case, obtained with values $c_1 = 3$ and $c_2 = 5$ (as in fig. 1) and $v_1 = 0.2$. If $v_2 < 2/c_2 = 0.4$, then the fixed point E^* attracts almost all the points of the phase space A. If v_2 is increased and the bifurcation value $2/c_2$ is crossed, also infinity becomes an attractor.

Hence, diverging trajectories can be obtained (see the Appendix). The basin of E^*, $\mathcal{B}(E^*)$, is then given by a subset of the phase space A. We start our numerical exploration just after this bifurcation: the situation shown in fig. 3a is obtained for $c_1 = 3$, $c_2 = 5$, $v_1 = 0.2$, $v_2 = 0.401$.

As in fig. 2, we represent $\mathcal{B}(E^*)$ by white points and $\mathcal{B}(\infty)$ is represented by the grey-shaded region.The boundary $\partial\mathcal{B}(\infty)$ separating $\mathcal{B}(E^*)$ from $\mathcal{B}(\infty)$ is given by the q_1-axis (denoted by ω_0 in fig. 3) and its preimages of any rank, denoted by ω_{-n} , $n > 0$ (in particular the set of rank-1 preimages ω_{-1} can be analytically computed, belonging to the parabola of equation $(1 - c_2v_2)(x + y)^2 + v_2x = 0$). Indeed, each coordinate axis is a trapping set, i.e. the points of a coordinate axis are mapped in the same axis by T, and the restriction of T to a coordinate axis is a linear unidimensional map. If we consider the q_1-axis, we have $T(q_1, 0) = (q_1', 0) = ((1 - c_1v_1q_1), 0)$. For the q_2-axis we have $T(0, q_2) = (0, q_2') = (0, (1 - c_2v_2q_2))$. Thus the point $Q = (0, 0)$ can be seen as a fixed point for both of the restrictions, which are attracting if $0 < c_iv_i < 2$, $i = 1, 2$. The union of the coordinate axes and all their preimages forms a trapping set: $F_{q_1} = \bigcup_{n=0}^{\infty} T^{-n}(\{q_2 = 0\})$ may be considered as the local stable set of the point Q for $0 < c_1v_1 < 2$ and the local stable set of the point $E_{q_1} = (\pm\infty, 0)$ on the Poincaré Equator when $c_1v_1 > 2$ (see the Appendix). Equivalently, $F_{q_2} = \bigcup_{n=0}^{\infty} T^{-n}(\{q_1 = 0\})$ can be considered as the local stable set of Q if $0 < c_2v_2 < 2$ and of the point $E_{q_2} = (0, \pm\infty)$ on the Poincaré Equator when $c_2v_2 > 2$.

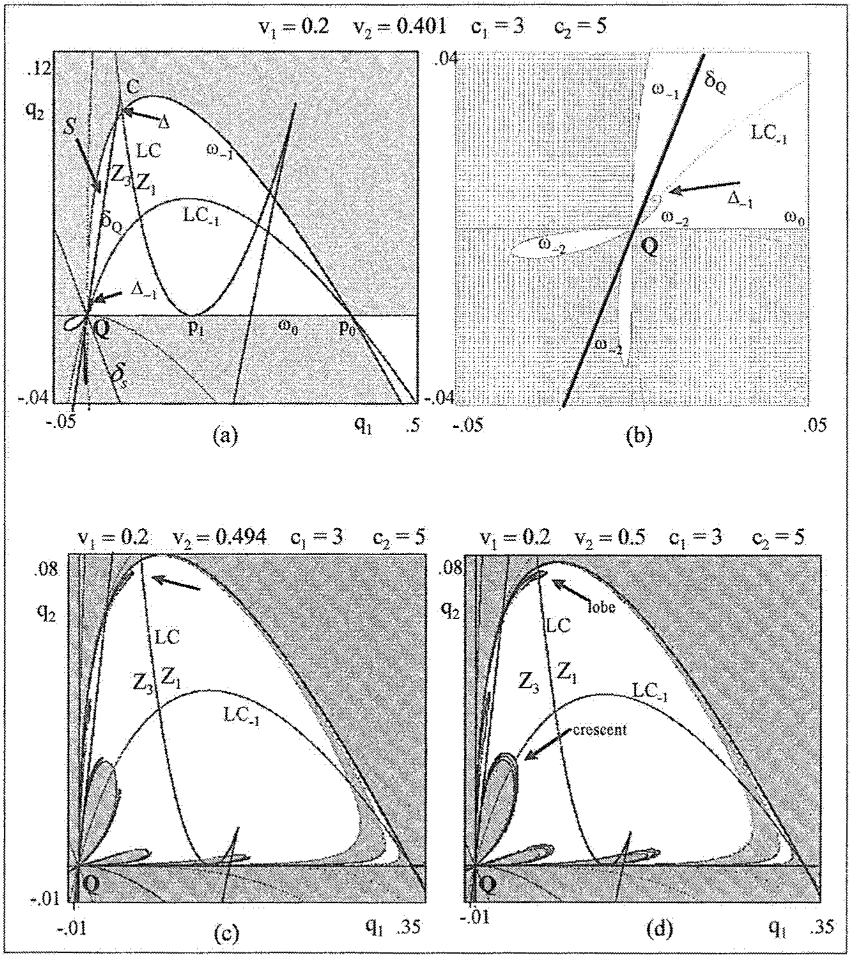

Figure 3.

In the situation shown in fig. 3a, the critical curve LC, together with δ_Q and ω_{-1}, bounds a small region, labeled by Δ. This region has three rank-1 preimages. The union of two of the three preimages of Δ, namely $T_1^{-1}(\Delta)$ and $T_2^{-1}(\Delta)$, forms a lobe issuing from the focal point $Q = (0,0)$ and entering inside the positive quadrant of the phase space, denoted by Δ_{-1} in fig. 3a. In the enlargement shown in fig. 3b the lobe $\Delta_{-1} = T_1^{-1}(\Delta) \cup T_2^{-1}(\Delta)$ is clearly visible, together with two lobes, which are rank-1 preimages of the region labelled by S. As $Q \in \delta_Q$, infinitely many gray lobes, as well as infinitely many white lobes, must issue from the focal point Q, as stated by the corollary given above. However, it is very difficult to display this complex structure graphically, because all these lobes are tangent to the coordinate axes (since

$m = 0$ or $m = \infty$ are the slopes associated with $u = 0$ in (6)). If the parameter v_2 is increased, the existence of these infinitely many lobes becomes more evident, as can be seen in fig. 3c. In this figure other new phenomena are evidenced: whenever a lobe Δ_{-k} crosses LC, its preimage Δ_{-k-1} includes the merging of two lobes on LC_{-1}. This can be seen by comparing the figures 3c and 3d, where the contact of the lobe indicated by the arrow with LC causes the merging of its preimages, with the accompanying creation of other particular structures of the basins called crescents in [1]. This causes a further restriction of the basin of E^*. This is even more obvious in fig. 4, where another evident merging of lobes related to a contact of a lobe with LC and a corresponding creation of a big crescent is shown. As the parameter v_2 is further increased, more and more lobes of $B(\infty)$ have a contact with LC, and this leads to an intermingled structure of "white and grey" regions. As a final remark, we mention that the creation of crescents, as the result of merging of lobes, is a peculiarity of noninvertible maps with focal points. In fact, it requires that a portion of the basin boundary cross a prefocal curve located in a region Z_k with $k > 1$, followed by a contact with a critical curve which causes the merging of the lobes.

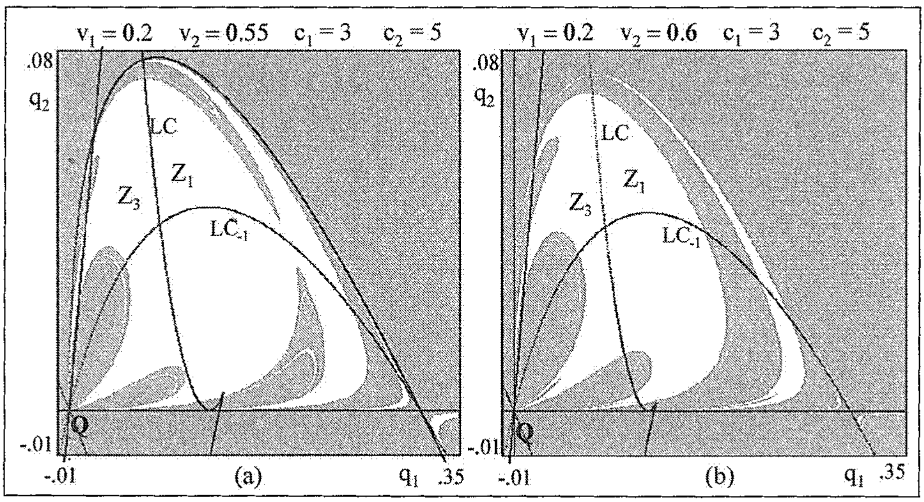

Figure 4.

4 Appendix. Study of the map on the Equator of Poincaré

The method of the "Poincaré Equator", commonly used in the study of ordinary differential equations of the plane (see [20]) can also be used for the study of divergent trajectories of two-dimensional maps (see [14]). Let $M = (q_1, q_2)$ be a point of the phase plane α of the map (2) and $M^*(u, v)$ the corresponding point on the plane α^* tangent to the Poincaré Sphere and perpendicular to the q_1 axis (see e.g. [14] p.232, or [20] p.219). The transformation

$$q_1 = \frac{1}{z} \quad q_2 = \frac{u}{z} \tag{7}$$

allows us to obtain the map whose trajectories are the projections of the trajectories of the map (2) on the plane α^*. After substitution of (7) into (2) we have

$$\begin{cases} z' = z\frac{(1+u)^2}{(1-c_1v_1)(1+u)^2+v_1uz} \\ \\ u' = u\frac{(1-c_2v_2)(1+u)^2+v_2z}{(1-c_1v_1)(1+u)^2+v_1uz} \end{cases} \tag{8}$$

The points of the Poincaré Equator, of equation $z = 0$, represent the locus of points at infinity (or improper points) of the plane α. From the first of (8) we deduce that the Poincaré Equator is invariant, since $z = 0$ implies $z' = 0$. The only fixed point on the Poincaré Equator is $X = (0, 0)$, which corresponds to the direction of q_1 axis. The Jacobian matrix of (8), evaluated on the Poincaré Equator, is the following triangular matrix

$$J_{\alpha^*}(0, u) = \begin{bmatrix} \frac{1}{1-v_1c_1} & 0 \\ \\ \frac{u(v_2(1-v_1c_1)-v_1u(1-v_2c_2))}{(1+u)(1-v_1c_1)} & \frac{1-v_2c_2}{1-v_1c_1} \end{bmatrix} \tag{9}$$

which becomes diagonal at the fixed point X, with eigenvalues $\frac{(1-v_2c_2)}{(1-v_1c_1)}$ and $\frac{1}{(1-v_1c_1)}$. The transformation (7) does not allow us to study the points at infinity in the direction of the q_2 axis. This difficulty is overcome by considering the transformation $q_1 = \frac{v}{z}$, $q_2 = \frac{1}{z}$ (see [20]) which gives the projection on the plane $\widehat{\alpha}$ tangent to the Sphere of Poincaré and perpendicular to the q_2 axis. The transformed map has the same form as (8) with the variable u substituted by v and by exchanging indexes 1 and 2. Also this map has the unique fixed point $Y = (0, 0)$, that represents the direction of the q_2 axis.

The nature of the fixed point X is determined by the eigenvalues of (9), that is, $\lambda_X^z = \frac{1}{1-v_1c_1}$, associated to the direction of the z axis, and $\lambda_X^u = \frac{1-v_2c_2}{1-v_1c_1}$, associated to the direction of the u axis (tangent to the Poincaré Equator). Analogously the nature of the fixed point Y is determined by the eigenvalues, $\lambda_Y^z = \frac{1}{1-v_2c_2}$, associated to the direction of the z axis, and $\lambda_Y^v = \frac{1-v_1c_1}{1-v_2c_2}$, associated to the direction of the v axis (tangent to the Poincaré Equator). For example the fixed point X is a stable node if $c_1v_1 > 2$ and $|1-c_2v_2| < |1-c_1v_1|$. Analogous conditions, obtained by exchanging the indexes, hold for the fixed point Y. Of course we are mainly interested in the direction z, indicating towards the interior of the Poincaré Equator. If

$$c_1 v_1 < 2 \quad \textit{and} \quad c_2 v_2 < 2 \tag{10}$$

both the fixed points are repelling in the z direction, i.e. toward the interior of the Poincaré Equator. Furthermore, even if cycles of period $k > 1$ exist on the Poincaré Equator, these are repelling in z direction if conditions (10) hold true. In fact the Jacobian matrix evaluated at a k-cycle, say C_k, located on the Poincaré Equator, is given by the product of k triangular matrices (9), which is a triangular matrix whose eigenvalue associated to the z direction is

$$\lambda^z_{C_k} = \left(\frac{1}{1 - c_i v_i}\right)^k \tag{11}$$

where the value of i is 1 or 2 depending on the transformation considered. Thus we can state that when conditions (10) are satisfied *the Poincaré Equator is repelling.*

References

[1] Bischi, G.I. , L. Gardini and C. Mira (1999). Maps with denominator. Part 1: some generic properties, International Journal of Bifurcation & Chaos, vol.9, n.1, 119-153.

[2] Nitzan, S. (1994): Modelling rent-seeking contest, European Journal of Political Economy, 10, 41-60.

[3] Baik, K.H. (1994): Effort levels in contests with two asymmetric players, Southern Economic Journal 61, 367-378

[4] Pérez-Castrillo, J.D. and T. Verdier (1993): A general analysis of rent-seeking games, Public Choice 73, 335-350.

[5] Nti, K.O. (1997): Comparative statics of contests and rent-seeking games, International Economic Review 38, 43-59.

[6] F. Szidarovszky and K. Okuguchi. On the Existence and Uniqueness of Pure Nash Equilibrium in Rent-Seeking Games, Games and Economic Behavior, 18 (1997) 135-140.

[7] Sargent, T.J. (1993) Bounded Rationality in Macroeconomics, Clarendon Press, Oxford

[8] R. Marimon. 1997. Learning from learning in economics, in D.M. Kreps and K.F. Wallis, eds., Advances in Economics and Econometrics: Theory and Applications, Volume I, Cambridge University Press, Cambridge, UK.

[9] Fudenberg, D., Levine, D.K., 1998. The Theory of Learning in Games, MIT Press, Cambridge, Massachusetts.

[10] F. Szidarovszky and K. Okuguchi. On a Dynamic Rent-Seeking Game, mimeo, University of Arizona, Department of Systems and Industrial Engineering, Tucson, AZ.

[11] L. Xu and F. Szidarovszky (1999) The Stability of Dynamic Rent-Seeking Games, International Game Theory Review, 1, 87-102.

[12] Okuguchi, K. and F. Szidarovszky (1999): The theory of oligopoly with multi-product firms, Second, Rev. and Enlarged Ed., Springer.

[13] Chiarella, C. and F. Szidarovszki (2000): On the Asymptotic Behavior of Rent-Seeking Games, mimeo, University of Arizona, Department of Systems and Industrial Engineering, Tucson, AZ.

[14] Gumowski, I. and Mira, C. (1980). Dynamique Chaotique, Cepadues Editions, Toulose.

[15] S.D. Flam. Oligopolistic Competition: from Stability to Chaos, in: F.Gori, L.Geronazzo and M.Galeotti (Eds.), Nonlinear Dynamics in Economics and Social Sciences, Lecture Notes in Economics and Mathematical Systems, 399, (Springer, 1993), 232-237.

[16] G.I. Bischi and A. Naimzada. Global Analysis of a Duopoly game with Bounded Rationality, Advances in Dynamic Games and applications, (Birkhauser, 1999), vol.5, 361-385.

[17] G.I. Bischi, L. Gardini and M. Kopel Analysis of Global Bifurcations in a Market Share Attraction Model, Journal of Economic Dynamics and Control, 24, pp. 855-879 (2000).

[18] Mira, C., Gardini, L., Barugola, A. and Cathala, J.C. (1996) Chaotic Dynamics in Two-Dimensional Noninvertible Maps, World Scientific, Singapore.

[19] R. Abraham, L. Gardini and C. Mira. Chaos in Discrete Dynamical Systems (a visual introduction in two Dimensions), Springer, 1996.

[20] Andronov, A.A., Leontovich, E.A., Gordon, I.I. and Maier, A.G. (1973). Qualitative Theory of Second-Order Dynamic Systems, Israel Program for Scientific Translations, John Wiley and Sons.